Influence of the Eu^{3+} luminescence center concentration on the properties of Gd_2O_3:Eu phosphor system obtained by aerosol synthesis

M.E.Rabanal[1*], C.Morales[1], J.M.Torralba[1], L.Mancic[2] and O.Milosevic[2]

[1]University Carlos III, Avda. Universidad 30, 28911 Leganes, Madrid, Spain,
[2]Institute of Technical Sciences of SASA, K.Mihajlova 35/IV, 11000 Belgrade, Serbia & Montenegro

Influence of the Eu^{3+} luminescence center concentration on the structural, morphological and spectroscopic properties of the powders obtained in accordance to the aerosol method was studied in this work. The processing route includes aerosol formation ultrasonically (resonant frequency 1.7MHz) from common gadolinium and europium nitrate solutions and control over the aerosol decomposition in a high-temperature (up to 1473K) tubular flow reactor. During decomposition, the aerosol droplets undergo evaporation/drying, precipitation and thermolysis in a dispersed phase and in a single-step process. Consequently, spherical, solid, agglomerate-free, submicron-sized particles with the crystallite sizes below 20nm were obtained. In order to control the particles crystal structure and to establish the conditions for the stabilization of the low-temperature gadolinia cubic phase, the process parameters like synthesis temperature, droplet/particle residence time and annealing temperatures were adopted. The particle morphology, phase and chemical structure were revealed in accordance to various analysis methods (XRD, SEM and EDS). Structural changes (crystallite size and microstrains) after powders thermal treatment were carried out using Koalariet-XFit program as the profile-matching tools. The results obtained and the mechanisms of ultrafine phosphor particles generation were discussed in terms of precursor chemistry, process parameters and luminescence properties.

[*] **Corresponding author.**
Tel.: +34 91 624 99 16

E-mail address: eugenia@ing.uc3m.es

Key words: spray pyrolysis, Gd_2O_3:Eu phosphor particles, luminescence, and structural analysis;

Introduction

The processing of advanced phosphor materials emphasizes the importance of ultrafine powder synthesis. Efficiency of light emission, caused by the interaction between atomic states associated with luminescence center and the host lattice material[1], is primary affected by the homogeneity in dispersion of activator ions. Additionally, superior luminescence properties were attained in phosphor particles having spherical morphology, submicrometer sizes and narrow particle size distributions[2,3]. Spray pyrolysis is one of the basic aerosol routes, which provides such structural properties in powder. It is relatively low cost, simple to manipulate and applicable to large-scale production[4]. In this process, a precursor solution is pulverized into mist and in the form of very fine droplets is carried into tubular flow reactor by means of compressed air. With adequate conditions, the precursor salts react to form the desired compound into the furnace. The starting chemical reactants, temperature regime and other processing parameters should be selected in way that prevents undesirable products formation. The properties of the powders depend greatly on the preparation conditions and can be easily tailored by adjusting of the parameters, making them suitable for a particular application[5].

Gadolinium oxide has been extensively used in many different applications[6,7]. When is activated by rare earths (ie. Eu^{3+} or Nd^{3+}), it became an effective crystal phosphor, presenting cathodo-luminescence and laser action[8]. In continuation of our previous studies on Gd_2O_3:Eu red phosphor material synthesis through spray pyrolysis[9-10], the goal of this paper is to investigate the influence of the Eu^{3+} luminescence center concentration on the structural, morphological and spectroscopic properties of the powders obtained under different temperature regime, residence time and annealing temperatures.

Experimental

The spray pyrolysis experimental set-up consists of an ultrasonic nebulizer with 3 transducers operated at 1.7MHz, quartz tube located inside a cylindrical furnace and particle collector. The fine drops of precursor solutions were carried out by the airflow regulated with a flow controller. The decomposition of the precursor salts was performed in two different temperature profiles (either at constant or increased temperature). The details of the established synthesis conditions and calculated droplet/particle residence time* are presented in Table 1. Two precursor solutions having the same overall concentration of nitrates (0.1mol/dm^3) were prepared by dissolving the appropriate amounts of $Gd(NO_3)_3x6H_2O$ and $Eu(NO_3)_3x6H_2O$ in order to obtain either 0.95:0.05 or 0.90:0.10 Gd:Eu molar ratio (as-prepared samples are denoted as S05 and S1, respectively). After synthesis, the powders were annealed isothermally at 1273-1473K in the chamber furnace in air, Table 1.

The crystal structure of the as prepared and thermally treated powders was analysed by X-Ray diffraction (XRD) collected in an automatic X´Pert Philips diffractometer, using a Cu K_α (λ=1.54056 Å) source operating at 40 kV and 30mA. Data were collected in the 2θ ranges from 15 to 60º, in step-scanning mode with a step of 0.02º and counting time (5-18s per step). All peak positions were used in the determination of precise microstructural parameters. Structural refinements were carried out using the Rietveld program Koalariet-Xfit [11]. Compositional homogeneity and particle morphology were analysed by scanning

electron microscopy (SEM, Hitachi S-800; SEM S-4500), and energy dispersive X-ray spectroscopy (EDX prime). Qualitative sample analyses were done in accordance to spot and area analysis. Particle size analysis was done by a laser particle size analyser (Malvern Master Sizer). Luminescence properties were measured with a sharp excitation spectra excitation wavelength of Ar laser (10mW) at 366nm on powdered samples. The wavelength measuring range was 500-700nm by using a conventional lock in amplitude and photomultimeters as a detector.

Results and Discussion

SEM photographs of powder samples S05 and S1 are shown on Figs.1 and 2, respectively. They implied formation of individual particle with spherical shape and filled morphology. Gradual increases of the decomposition temperature in one of the applied temperature regimes during synthesis results in the same shrinkage and densification effect of spherical particles originated through volume precipitation. Smooth particle surface is characteristic of as-prepared powders, while rough surface is detectable after annealing due to the additional promotion of the crystallization process. Narrow particle size distribution is determined for all powdered samples. The mean particle size in as-prepared powder (sample S05) is determined to be 800nm, Fig.3a. Comparing the particle sizes derived from the SEM photomicrographs, it can be noticed that particle size slightly decrease during thermal treatments as a consequence of additional densification, but morphology and shape of the particles remain the same. Only for the sample treated at the highest temperature (1473K. Fig.1d), the initial stage of interparticle sintering is noticeable through particle bonding and neck formation.

According to the EDS area analysis for serial S05, the concentration of europium in as-prepared powdered sample for particle sizing 1.64μm is 5.46 at% (denoted as rectangle at Fig.1a and presented at Fig.3b). After annealing, europium ion concentration is determined as to be 2.99 at% for particle having with the diameter of 1.1 μm (analyzed area is rectangle marked at Fig.1d). Qualitative and semiquantitative EDS spot analysis is performed in randomly chosen particles in samples from serial S1, as well. Results obtained imply slightly changeable content of activator ion in different sized particles, but the uniformity of its presence, ranged from 2.1 to 4.4at%, is determined for all samples.

XRD phase analyses implied the presence of the cubic Gd_2O_3 phase (file card 43-1014) in all samples. Beside Gd_2O_3, another cubic phase is evident for as-prepared powders (12wt% in S1). The latter phase is structurally similar to the $Gd_2Te_6O_{15}$ (SSI) (file card 37-1400), and corresponds to the intermediate solid solution with disordered CaF_2 type structure in which Eu^{2+} ions can exchange Te^{4+} or Eu^{3+} ions can substitute Gd^{3+}. Extensive ions exchange is highly possible because of close ionic radius match: for Eu^{2+} - 0.112nm; Te^{4+} - 0.111nm,; Eu^{3+} - 0.095nm; Gd^{3+} - 0.094nm (all having octahedral coordination). It seems that this intermediate phase evolution is additionally influenced by the synthesis conditions that enable partially Eu^{3+} ion reduction to Eu^{2+}, due to the oxygen depletion at the particle surface caused by high concentration of adsorbed nitrogen. The presence of nitrogen is evident by EDS analysis of the as-prepared particle, Fig 3b. The corresponding peak ratio of SSI (111) ($2\theta \approx 27.5°$)-to-cubic gadolinium oxide (222) ($2\theta \approx 28.5°$)- phase, $I_{SSI\,(111)}/I_{(222)}$ is 4.7 and 0.33, for the as-prepared powder samples S05 and S1, respectively. The intermediate solid solution phase (SSI) disappeared after annealing above 673K[10].

Well- developed peaks of cubic gadolinia are evident in both as-prepared samples S05 and S1 after annealing. Based on this spectra peaks fitting have been done in order to provide some of the main crystallographic data. Typical XRD pattern of pure Gd_2O_3:Eu phase obtained after powders annealing together with the resulting difference curve is presented at Fig.4a. The estimated values of the cell parameters for the cubic gadolinium oxide phase, presented in Table 1, imply the tendency of crystal cell increase with increase of thermal treatment temperature.

The structural changes expressed through average crystallite size and lattice microstrains, presented in Table 1, imply gradual increases of crystallinity, as well as, decrease of microstrains with increase of the annealing temperature. The main feature of as-prepared particles is the presence of the small primary crystallites. The value of 16.2nm, determined for sample S1, confirms that although SEM reveals visually uniform particle surface, particles are characterized with composite structure and presence of smaller grains. Promoted crystallite growth is evident in thermally treated samples (S05-1: 27.9 nm, S05-2: 49.5 nm, S1-1: 60.7 nm, S1-2: 54.4 nm). Particle surface roughness, evident on Fig. 1c, results from the thermally induced crystallite growth, collision and aggregation into clusters.

The relationship among the crystal cell parameter, thermal treatment temperature and europium content, determined as the mean value of EDS spot analysis data obtained in randomly chosen particles, is presented at Fig.4b. Gradual increase of crystal cell with both temperature and Eu at % could be associated with the Eu^{3+} ions incorporation into gadolinium oxide matrix, since it is a thermally induced diffusion process.

The substitution of Gd^{3+} lattice sites with europium ion in gadolinium oxide matrices is additionally confirmed for the powder samples serial S05 by red emission and the appearance of two dominant peaks at 615 and 624nm, Fig.5a. The emission band at 624 nm is probably related to the intermediate solid solution phase (SSI), as revealed by XRD. Similar results are reported previously for the spray pyrolysed gadolinia-doped-europia prepared at 1173K[10]. The sharp emission band peaking at 612nm is detected for the thermally treated samples having the highest intensity for the sample S05-2. This emission line corresponds to the $^5D_0 \rightarrow {}^7F_2$ Eu^{3+} transition for C_2 crystallographic site in gadolinium oxide matrix[12].

On Fig.5b, the emission energy is presented as a function of the calculated Eu-Eu distance for different Eu^{3+} ion doping concentration, determined as the mean value of corresponding EDS spot analysis performed in randomly chosen particles. Namely, based on the presumption that luminescence intensity is influenced by the Eu^{3+} ions concentration substituted on Gd^{3+} lattice sites in gadolinium oxide matrix, the average distance ($d_{Eu\text{-}Eu}$) between centers of luminiscence could be calculated from the average volume occupied by Eu atoms, assuming ideal distribution[13].

$$d_{Ce\text{-}Ce} = 2[V_{Eu}/ (4/3\pi)]^{1/3} \quad (1)$$

and

$$V_{Eu} = (1/N_a)(V_m/X_{Eu}) \quad (2)$$

where: V_m: is a molar volume calculated from the weighed-out composition; N_a: is Avogadro number; X_{Ee}: is Eu^{3+} concentration.

Fig 4b, confirms the results reported for other systems[13,14], where higher content of activator ion reduces the distance between luminescent centers and increase the intensity of emission.

Conclusions

Submicron-sized and exceptionally well structurally and morphologically defined nanophased Gd_2O_3:Eu phosphor particles were prepared by spray pyrolysis method. All produced particles are spherical and nonagglomerated with uniform particle size distribution. It was shown that uniformity of phase content influences luminescence causing the appearance of two dominant peaks on 615 and 625 nm for as prepared powder, while sharp emission band at 612 nm is associated with single cubic gadolinium structure completely formed after additional thermal treating. The structural changes expressed through the crystallite size and lattice microstrains imply increase of crystallinity together with the retaining of the desired morphology characteristics resulting in pronounced luminescence properties. All those characteristics together with the high reactivity of particles produced through spray pyrolysis make them suitable for obtaining good packing densities in practical display applications.

ACKNOWLEDGEMENTS:

This research was financially supported through the NEDO International Joint Research Grant Program 01MB7: "Wetability of solid by liquid at high temperatures", as well as Republic of Serbia Science Foundation No.1832.

References

[1] E.J.Kim, Y.C.Kang, H.D.Park and S.K.Ryu, UV and VUV characteristics of $(YGd)_2O_3$:Eu phosphor particles prepared by spray pyrolysis from polymeric precursors, Mat.Res.Bull., 38, 3 (2002) 515-524.
[2] T.Hirai, T.Hirano, I.Komasawa, Preparation of $Gd_2O_3:Eu^{3+}$ and $Gd_2O_3S:Eu^{3+}$ phosphor fine particles using an emulsion liquid membrane system, J.Colloid Interface Sci., 253 (2002) 62-69.
[3] Y.Q.Zhai, Z.H.Yao, M.D.Qiu, B.S.Liu and X.L. Dai, Synthesis and luminescent properties of Gd_2O_3:Eu nanocrystalline using EDTA complexing sol-gel process, Indian Journal of Chemistry A, 43, 1 (2004) 71-75.
[4] T.L.Ward, T.T.Kodas and A.H.Carim, Powder characteristics and sintering behavior of Ag-doped $YBa_2Cu_3O_{7-x}$ produced by aerosol decomposition, J.Mater.Res., 7 (1992) 827-835.
[5] H.E.Esparza-Ponce, A.Reyes-Rojas, W.Antúnez-Flores and M.Miki-Yoshida, Synthesis and characterization of spherical calcia stabilized zirconia nano-powders obtained by spray pyrolysis, Mat.Sci.Eng. A, 343 (2003) 82-88.
[6] H.J.Seifert, F.Aldinger, U.Kolitsch, Phase relationships in the system Gd_2O_3-Al_2O_3-SiO_2, J.Alloys Compd. 257 (1997) 104-114.
[7] G.A.M.Hussein, Formation, characterization, and catalytic activity of gadolinium oxide. Infrared spectroscopic studies, J.Phys.Chem., 98, 38 (1994) 9657-9664.
[8] A.Brenier and G.Boulon, Laser heated pedestal growth and spectroscopic investigations of Nd^{3+}-doped Gd_2O_3 single crystal fibres, J.Lumin., 82 (1999) 285-289.

[9] O. Milosevic, L.Mancic, B. Jordovic, R. Maric, S. Ohara and T. Fukui, Processing of Gd2O3:Eu phosphor particles through aerosol route, J.Mat.Proc.Tech., 143-144 (2003) 501-505
[10] O.Milosevic, R,Maric, S.Ohara and T.Fukui, Aerosol synthesis of phosphor based on Eu3+ activated gadolinium oxide matrices, Ceramic Transactions, Vol.112, Ceramic Processing Science, VI, ed. American Ceramic Society, 2001,101-106
[11] R.W.Cheary and A.A. Coelho, Programs XFIT and FOURYA, CCP14 Powder diffraction Library-Daresbury Laboratory, Warriington, England (1996).
[12] M.Buijs, A.Meyernik and G. Blasse, Energy transfer between Eu^{3+} ions in a lattice with two different crystallographic sites: Y_2O_3 : Eu^{3+}, Gd_2O_3 : Eu^{3+} and Eu_2O_3, J. of luminescence, 37 (1987), 9-20
[13] D.de Graaf, H.T.Hintzen, G.de With, The influence of the composition on the luminescence of Ce(III)-Ln-Si-Al-O-N glass (Ln=Sc, Y, La, Gd), J. of Luminescence, 104 (2003) 131-136.
[14] G. del Rosario, S.Ohara, L.Mancic and O.Milosevic, Characterization of YAG:Ce powders thermal treated at different temperatures, App.Surf.Sci., accepted for publication.

Table 1. Synthesis conditions and structural characteristic of as-prepared and annealed samples

Sample	Airflow rate (dm^3/min)	Residence time* in furnace or on T_{max} (s)	Synthesis or annealing temperature(K) and time (h)	Crystallite size (nm) and microstrain (%)	Cell parameter (Å)
S05	1.5	34 / 16	473 / 873 / 1173	-	-
S05-1			1073 – 24	27.9 – 0.079	10.8219
S05-2			1473 – 8	49.5 – 0.001	10.8293
S1	1.5	84 / 31	973	16.2 – 1.183	10.8040
S1-1			1073 – 12	60.7 – 0.233	10.8212
S1-2			1173 – 12	54.4 – 0.214	10.8244
S1-3			1273 – 12	-	-

* calculated from the airflow rates and the geometry of the reactors

Figure Captions:

Figure 1. SEM photomicrographs of Gd_2O_3:Eu particles prepared through spray pyrolysis: a) S1 b) S1-1 c) S1-2 d) S1-3.

Figure 2. SEM photographs of Gd_2O_3:Eu particles prepared through spray pyrolysis: a) S05 b) S05-1 c) S05-1 d) S05-2.

Figure 3. a) Particle size distribution in sample b) S05 EDS area analysis of S05

Figure 4. a) Typical XRD pattern of Gd_2O_3:Eu powder prepared through spray pyrolysis after additional thermal treatment b) Gd_2O_3:Eu cell parameter vs. determined Eu^{3+} ion doping concentration (EDS). Line is drawn as a guide for the eye.

Figure 5. a) Photoluminescence intensities of Gd_2O_3 Eu particles b) Emission energy as a function of the calculated Eu-Eu distance for determined Eu^{3+} ion doping concentration (EDS).

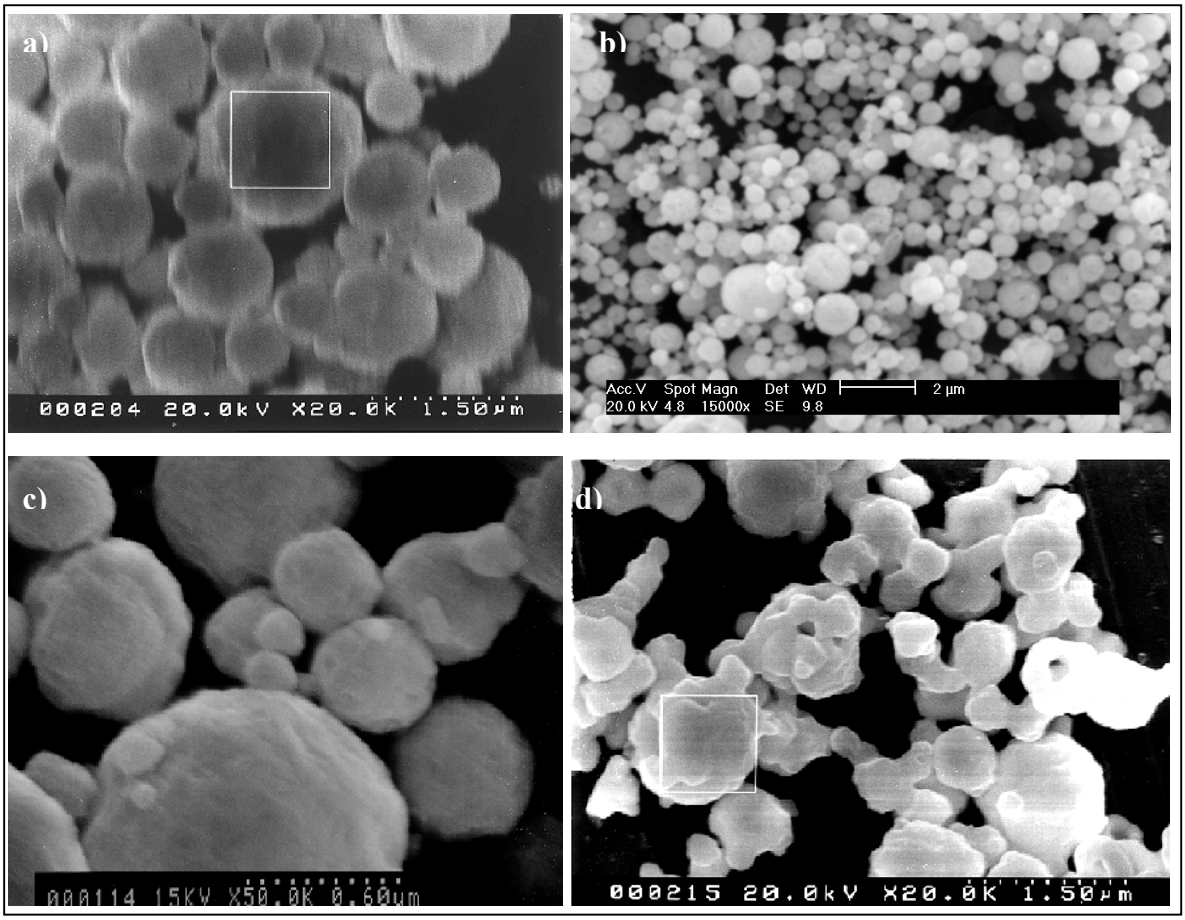
a)
000204 20.0kV X20.0K 1.50µm
b)
Acc.V Spot Magn Det WD 2 µm
20.0 kV 4.8 15000x SE 9.8
c)
000114 15KV X50.0K 0.60µm
d)
000215 20.0kV X20.0K 1.50µm

Figure 1.

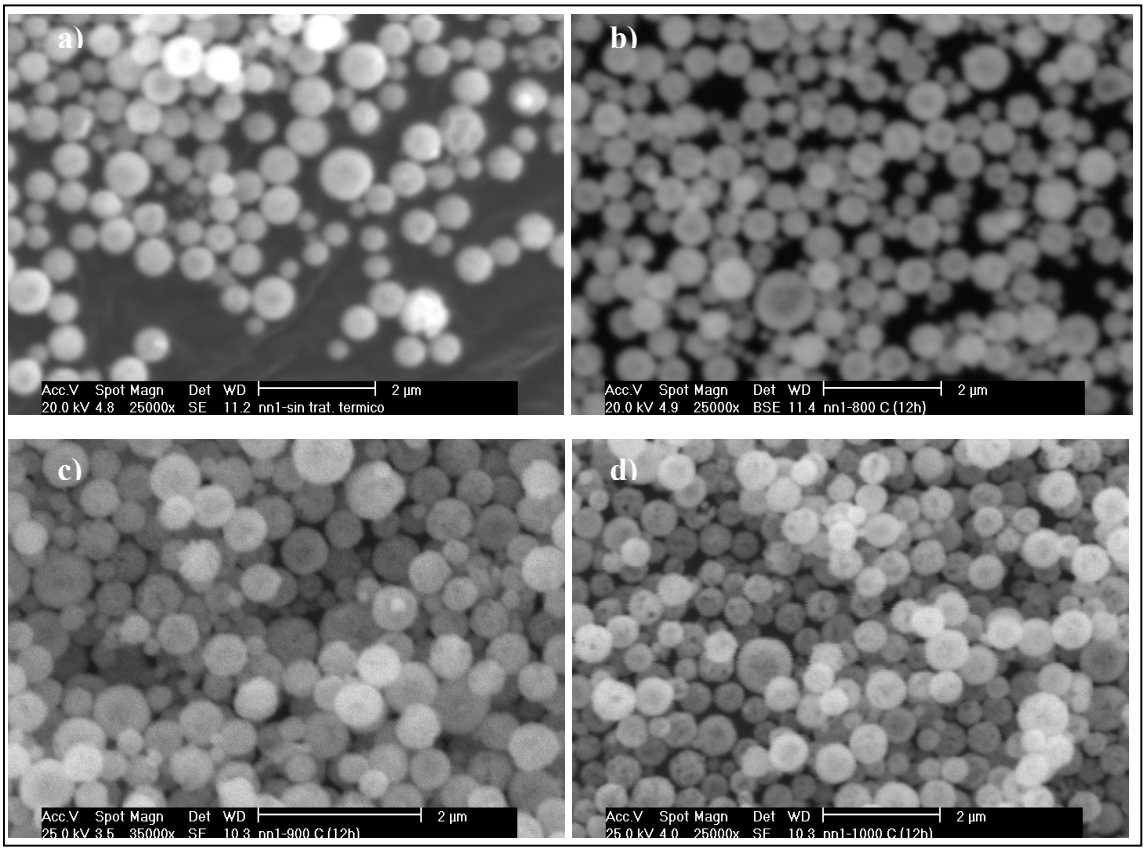
a)
Acc.V Spot Magn Det WD 2 µm
20.0 kV 4.8 25000x SE 11.2 nn1-sin trat. termico
b)
Acc.V Spot Magn Det WD 2 µm
20.0 kV 4.9 25000x BSE 11.4 nn1-800 C (12h)
c)
Acc.V Spot Magn Det WD 2 µm
25.0 kV 3.5 35000x SE 10.3 nn1-900 C (12h)
d)
Acc.V Spot Magn Det WD 2 µm
25.0 kV 4.0 25000x SE 10.3 nn1-1000 C (12h)

Figure 2.

b)

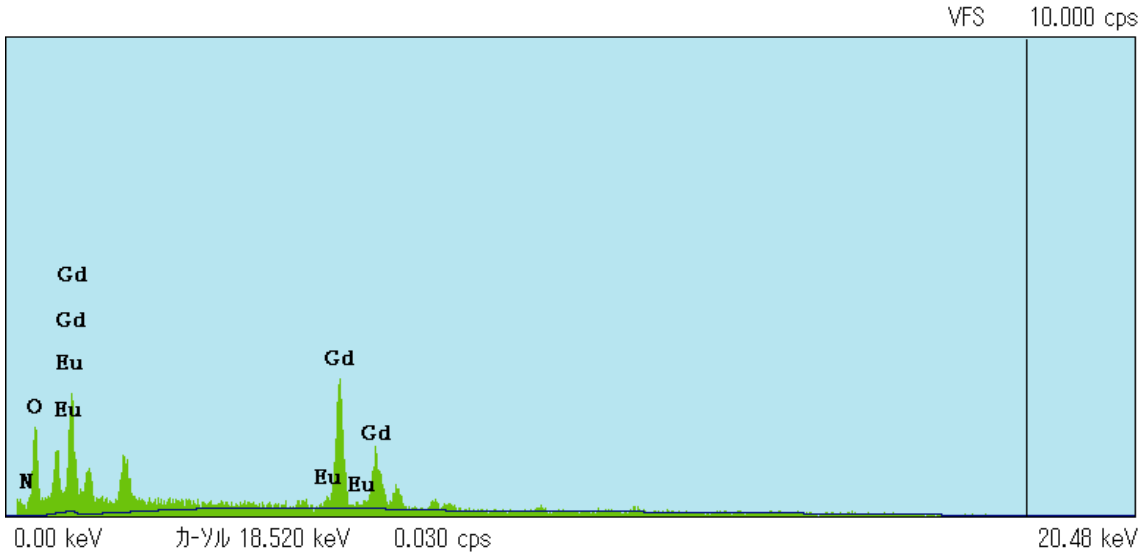
VFS
10.000 cps
Gd
Gd
Eu
O
Eu
Gd
Gd
N
Eu
Eu
0.00 keV
カーソル 18.520 keV
0.030 cps
20.48 keV

a)

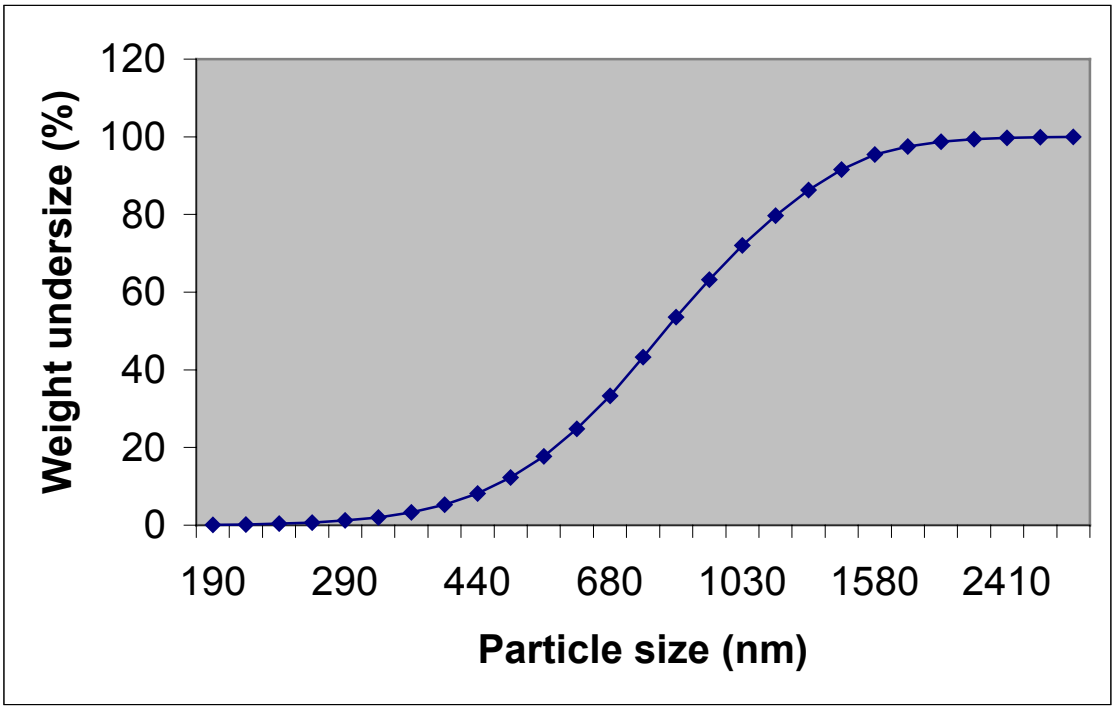
Weight undersize (%)
120
100
80
60
40
20
0
190
290
440
680
1030
1580
2410
Particle size (nm)

Figure 3.

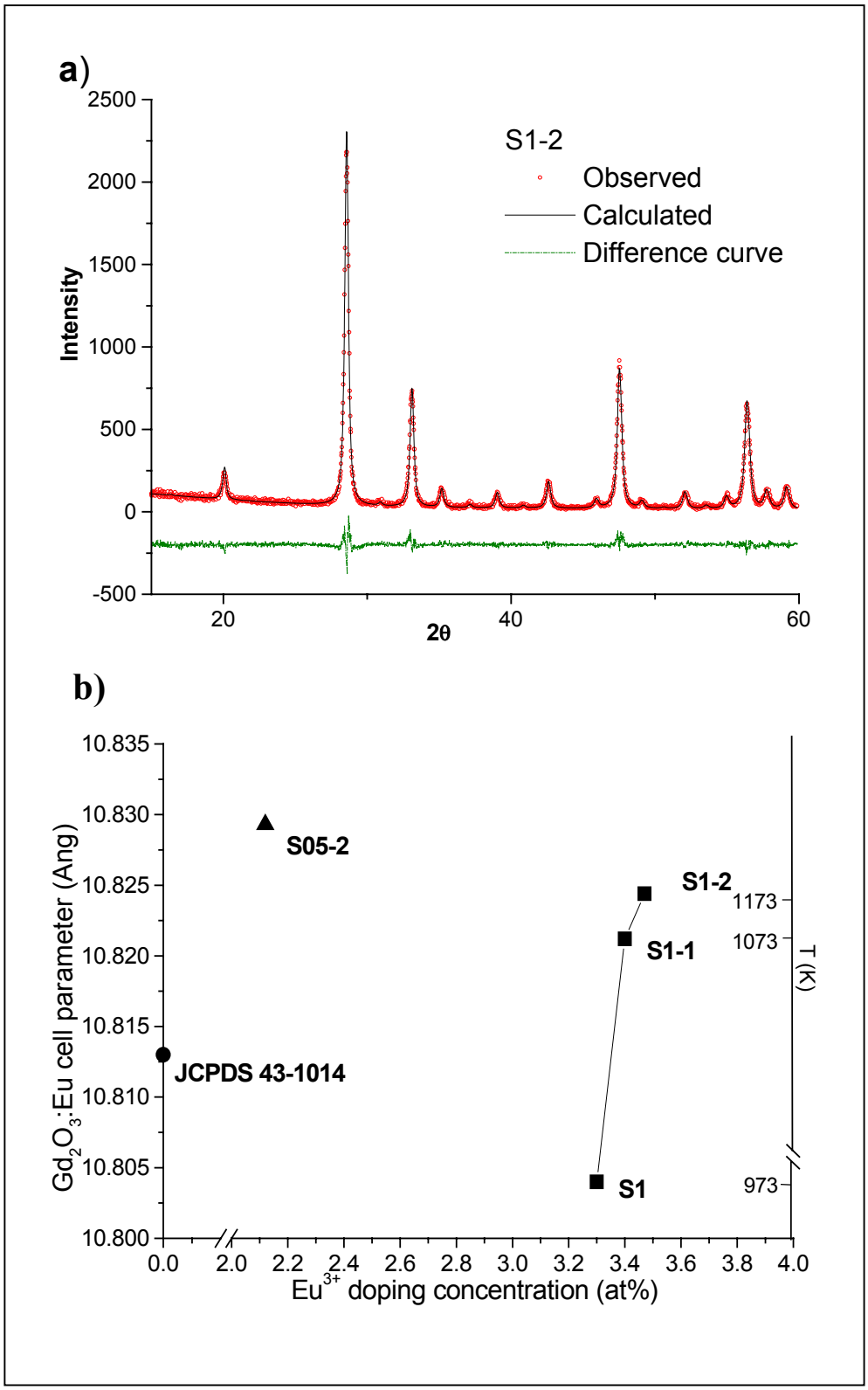
a)
S1-2
Observed
Calculated
Difference curve
Intensity
2θ
b)
S05-2
S1-2
S1-1
S1
JCPDS 43-1014
T (K)
1173
1073
973
Gd2O3:Eu cell parameter (Ang)
Eu3+ doping concentration (at%)

Figure 4.

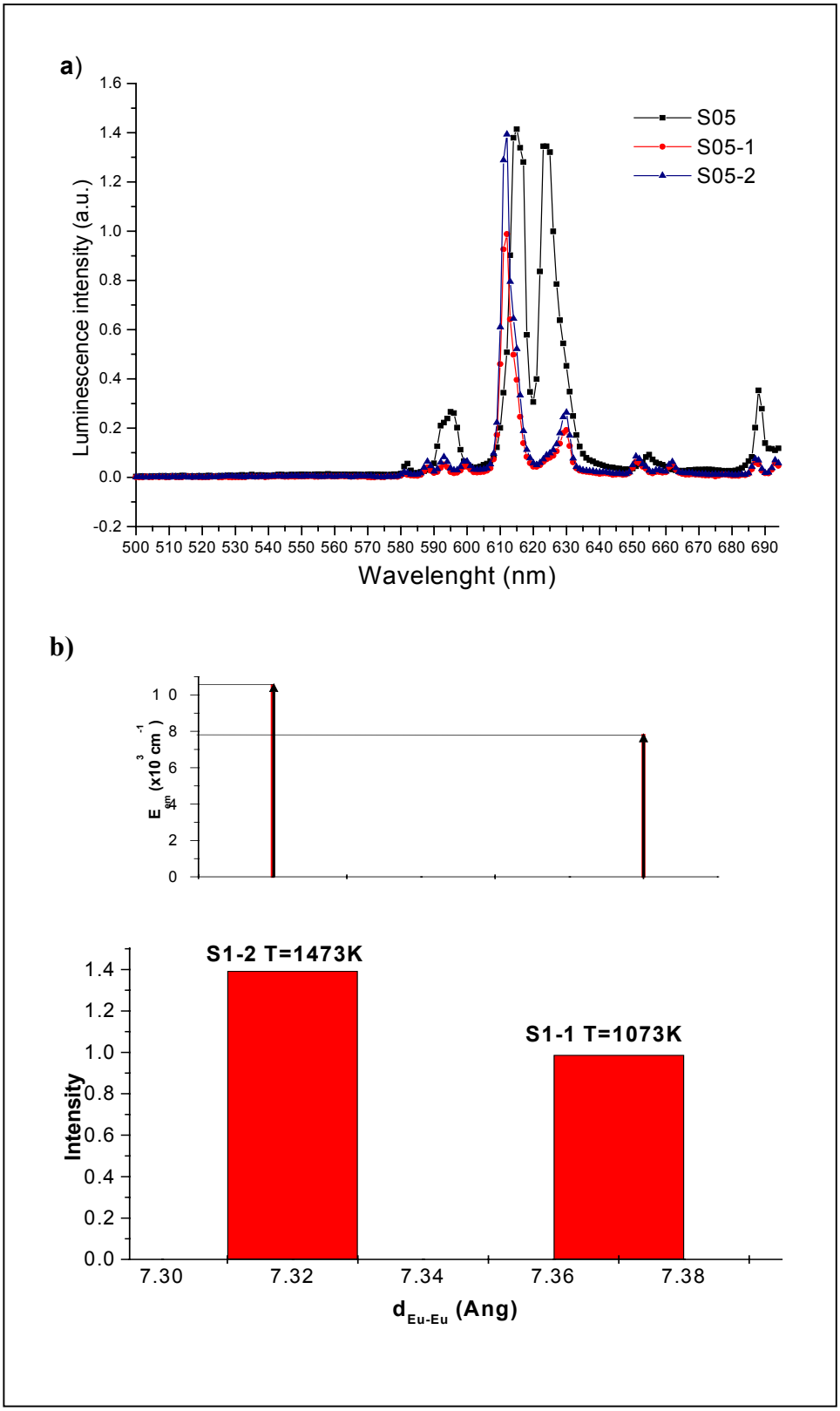
a)
Luminescence intensity (a.u.)
Wavelenght (nm)
S05
S05-1
S05-2
b)
S1-2 T=1473K
S1-1 T=1073K
Intensity
d Eu-Eu (Ang)

Figure 5.